Supplementary information

# Chain-Length Dependence of Propagation Rate Coefficient for Methyl Acrylate Polymerization at 25 °C Investigated by PLP-SEC Method.

*Anatoly N. Nikitin[1*], Eva Dušička[2], Igor Lacík[2,3], Robin A. Hutchinson[4]*

[1]Institute on Laser and Information Technologies of Russian Academy of Sciences – Branch of Federal Scientific Research Center "Crystallography and Photonics" of Russian Academy of Sciences, Svyatoozerskaya 1, 140700 Shatura, Moscow Region, Russia

[2]Polymer Institute of the Slovak Academy of Sciences, Dúbravská cesta 9, 845 41 Bratislava, Slovakia

[3]Centre for Advanced Materials Application of the Slovak Academy of Sciences, Dúbravská cesta 9, 845 11, Bratislava, Slovakia

[4]Department of Chemical Engineering, Dupuis Hall, Queen's University, Kingston, Ontario K7L 3N6, Canada

E-mail corresponding authors: anatoly_nikitin@mail.ru

## 1. Simulation of bulk methyl acrylate PLP at 25 °C.

### 1.1. The FM-PREDICI model

The free-radical polymerization of methyl acrylate (MA) at 25 °C is modeled in the PREDICI package[1] combining the basic set of reactions presented in Scheme S1 ((i)-(iii), (vi), (viii) and (xi)), with the additional mechanisms ((iv)-(v), (vii), (ix)-(x), (xii)-(xiii)) associated with the formation of midchain radicals (MCRs) arising from backbiting (iv) that results in a short chain branch (+SCB). As presented in Scheme S1, I and M are the initiator and the monomer, $\lambda$ is the initiation efficiency, $R_0$ are the primary radicals, $\mathbf{R}_i^s$ and $\mathbf{R}_i^t$ are the secondary and midchain (or tertiary) radicals with chain length i, and $P_i$ is dead polymer with chain length i. The model is referred to as the **f**ull **m**odel-PREDICI (FM-PREDICI) in this publication.

**Scheme S1.** Mechanisms of methyl acrylate polymerization at 25 °C.

**Initiation**

$$I \xrightarrow{h\nu} 2\lambda R_0 \quad \text{(i)}$$

$$R_0 + M \xrightarrow{k_i} R_1^s \quad \text{(ii)}$$

**Propagation**

$$R_i^s + M \xrightarrow{k_p^i} R_{i+1}^s \quad \text{(iii)}$$

**Backbiting**

$$R_i^s \xrightarrow{k_{bb}} R_i^t \quad \text{(iv)}$$

**Addition to midchain radical**

$$R_i^t + M \xrightarrow{k_p^t} R_{i+1}^s\,(+SCB) \quad \text{(v)}$$

**Chain transfer to monomer**

$$R_i^s + M \xrightarrow{k_{tr,M}^s} P_i + R_1^s \quad \text{(vi)}$$

$$R_i^t + M \xrightarrow{k_{tr,M}^t} P_i + R_1^s \quad \text{(vii)}$$

**Termination by combination**

$$R_i^s + R_j^s \xrightarrow{k_{tc}^{ss}(i,j)} P_{i+j} \quad \text{(viii)}$$

$$R_i^s + R_j^t \xrightarrow{k_{tc}^{st}(i,j)} P_{i+j} \quad \text{(ix)}$$

$$R_i^t + R_j^t \xrightarrow{k_{tc}^{tt}} P_{i+j} \quad \text{(x)}$$

**Termination by disproportionation**

$$R_i^s + R_j^s \xrightarrow{k_{td}^{ss}(i,j)} P_i + P_j \quad \text{(xi)}$$

$$R_i^s + R_j^t \xrightarrow{k_{td}^{st}(i,j)} P_i + P_j \quad \text{(xii)}$$

$$R_i^t + R_j^t \xrightarrow{k_{td}^{tt}} P_i + P_j \quad \text{(xiii)}$$

The kinetic parameters for MA polymerization at 25 °C presented in Table S1 are taken primarily from Kattner and Buback,[2] with the fraction of termination by combination vs. disproportionation assumed to be the same as for butyl acrylate (BA) bulk polymerization.[3] Designating the fraction of termination by disproportionation as δ, the values are $\delta_{ss}$ = 0.1 (for termination of secondary radicals), $\delta_{st}$ = 0.7 (for cross-termination between secondary and tertiary radicals), and $\delta_{tt}$ = 0.9 ( for termination of tertiary radicals). The rate coefficient of termination for tertiary radicals ($k_t^{tt}$) of MA polymerization at 25 °C is assumed not to be chain-length dependent, and set at a value twice higher than that for BA,[3] as the termination rate coefficient of secondary radicals for MA polymerization is higher than that of BA

polymerization at the same conditions.[2] For the same reason, the initiation rate coefficient for MA polymerization ($k_i$) is chosen to be higher than the one for BA polymerization presented in.[4] The CLD propagation rate coefficient for short and long radicals is described according to Equations (1) and (2) in the manuscript.

**Table S1.** Kinetic rate coefficients used for the FM-PREDICI simulation of MA polymerization at 25 °C

| Coefficients | | Values $L \cdot mol^{-1} \cdot s^{-1}$ or $s^{-1}$ | Reference |
|---|---|---|---|
| $k_i$ | | $3 \times 10^5$ | this work |
| $k_p^L$, Equation (1) | $i_{1/2}$ | 1 | [5] |
| | $C_1$ | 10 | [5] |
| | $k_p^\infty$ | 13 130 | [6] |
| $k_p^L$, Equation (2) | $k_p^0$ | 26 000 | this work |
| | $\beta$ | 0.1 | |
| $k_p^t$ | | 18 | [2] |
| $k_{bb}$ | | 229 | |
| $k_t^{ss}(i,j) = \left(k_t^{ss}(i,i) k_t^{ss}(j,j)\right)^{0.5}$ | $k_{tc}^{ss}(1,1)$ | $1.55 \times 10^9$ | |
| | $k_{td}^{ss}(1,1)$ | $1.72 \times 10^8$ | |
| | $\alpha_s$ | 0.8 | |
| | $\alpha_L$ | 0.21 | |
| | $L_f$ | 36 | |
| $k_t^{st}(i,j) = \left(k_t^{st}(i,i) k_t^{st}(j,j)\right)^{0.5}$ | $k_{tc}^{st}(1,1)$ | $2.0 \times 10^8$ | |
| | $k_{td}^{st}(1,1)$ | $4.64 \times 10^8$ | |
| | $\alpha_s$ | 0.8 | |
| | $\alpha_L$ | 0.21 | |
| | $L_f$ | 36 | |
| $k_{tc}^{tt}$ | | $3.8 \times 10^5$ | this work |
| $k_{td}^{tt}$ | | $3.4 \times 10^6$ | |

## 1.2. The 3D model

As previously summarized,[7] the kinetic scheme assumed for the 3D simulation consists of reactions (i)-(iii), (viii) and (xi) of Scheme S1, without consideration of CLD kinetic parameters. However, the variation of temperature, and initiator and monomer concentrations with time and in space are accounted for when calculating the resulting polymer molar mass distribution (MMD). The additional parameters required by the 3D model applied to the simulation of MA polymerization are presented in Table S2.

**Table S2.** The parameters used for the 3D simulation of MA polymerization at 25 °C

| Parameter | Value | Reference |
|---|---|---|
| Heat of polymerization, $-\Delta H_p$ kJ·mol$^{-1}$ | 81 790 | [8] |
| Specific heat, $C_p^M$ J·kg$^{-1}$·°C$^{-1}$ | 2 000 | [8] |
| Conductivity, $\lambda_M$ W·m$^{-1}$·K$^{-1}$ | 0.159 | [9] |
| Density, $\mu_T$ g·cm$^{-3}$ | 0.9471 | [9] |
| Activation energy for $k_p$, $E_a(k_p)$ kJ·mol$^{-1}$ | 17.3 | [6] |
| Pre-exponential factor for $k_p$, $A(k_p)$ L·mol$^{-1}$·s$^{-1}$ | $1.41\times10^7$ | [6] |
| Activation energy for $k_t$, $E_a(k_t)$ kJ·mol$^{-1}$ | 9.0 | [10] |
| Pre-exponential factor for $k_t$, $A(k_t)$ L·mol$^{-1}$·s$^{-1}$ | $3.5\times10^{10}$ | this work |

## 1.3. Analytical expressions for classical scheme (AECS) of free radical polymerization

Analytical expressions derived previously[11] for the classical (ideal) scheme of polymerization (i.e., consisting of reactions (i)-(iii), (viii) and (xi) of Scheme S1) have been used to simulate MMDs produced by PLP-SEC (AECS model). The mode of termination was chosen to be $\delta = 0.1$. The values of $y = k_p[M]t_d$ and $x = (\rho k_t t_d)^{0.5}$ (where $k_p$ and $k_t$ are the chain-length independent propagation and termination rate coefficients, [M] is the monomer concentration, $t_d$ is the pulse separation time, $\rho$ is the concentration of radicals produced by a pulse) are known[12] to control the shape of distribution under pseudostationary polymerization; $k_p$ and $x$ are varied to fit distributions calculated by the 3D simulation.

**Table S3.** Output values of β and $k_p^0$ estimated using Approaches 1 and 3 after using the AECS model to fit MMDs calculated by the 3D simulation of bulk MA PLP at 25 °C with different pulse repetition rates (p.r.r.) and numbers of pulses ($N_p$). In addition, the chain length corresponding to the maximum of the first peak in MMD ($L_1^{max}$), $h_2^{inf}/h_1^{max}$ ratios, SEC broadening parameters (σ), and mode of termination (δ) used in the AECS model fit are systematically varied, and an additional fit is made using the FM-PREDICI model.

| Figure | Approach | p.r.r. Hz | Varied parameter | β | $k_p^0$ L·mol$^{-1}$·s$^{-1}$ |
|---|---|---|---|---|---|
| Figure 2 | 1 | 500 | $N_p$ = 100 | –0.00033 | 13 270 |
| | | | 200 | 0.001 | 13 530 |
| | | 250 | 100 | 0.0033 | 13 560 |
| | | | 200 | 0.0043 | 13 860 |
| | 3 | 500, 250 | 100, 100 | 0.0070 | 13 870 |
| | | | 100, 200 | 0.0088 | 14 020 |
| | | | 200, 100 | 0.0057 | 13 920 |
| | | | 200, 200 | 0.0076 | 14 090 |
| Figure S3 | 1 | 500 | $L_1^{max}$ = 229 | –0.001 | 13 200 |
| | | | 332 | –0.00033 | 13 270 |
| | | | 364 | 0.0 | 13 290 |
| Figure S4 | 1 | 500 | $h_2^{inf}/h_1^{max}$ = 0.707 | 0.0020 | 13 360 |
| | | | 0.672 | –0.00033 | 13 270 |
| | | | 0.641 | –0.0017 | 13 140 |
| Figure S5 | 1 | 500 | σ = 0.035 | 0.0074 | 13 660 |
| | | | 0.04 | –0.00033 | 13 270 |
| | | | 0.045 | –0.0059 | 12 980 |
| Figure S6 | 1 | 500 | δ = 0.0 | –0.00922 | 12 690 |
| | | | 0.1 | –0.00033 | 13 270 |
| | | | 0.2 | 0.0084 | 13 810 |
| | | | 0.5 | 0.0251 | 14 980 |
| | | | 1.0 | 0.0351 | 15 690 |
| Figure S7 | 1 | 500 | AECS | –0.00033 | 13 270 |
| | | | FM-PREDICI | 0.0169 | 14 740 |

**Table S4.** Parameters determined from analysis of the MMDs calculated for bulk MA PLP at 25 °C for different pulse repetition rates (p.r.r.) by the AECS and FM-PREDICI models assuming different extents of CLD $k_p$ of long chain radicals (β and $k_p^0$). Tabulated values include log$M_1$ and log$M_2$ corresponding to the first two maxima from the MMD first derivative, the chain length ratio $L_1^{LIP}/L_2^{LIP}$ ($L_1^{LIP} = M_1/M_0$ and $L_2^{LIP} = M_2/M_0$, $M_0$ is monomer molar mass), the values of $L_1^{max}$ (the chain length corresponding to the maximum of the first peak) and $h_2^{inf}/h_1^{max}$ (described in the text) used to characterize the shape of the distribution, and correction factors $g_1^c$ and $g_2^c$ estimated from the simulated distribution.

| p.r.r Hz | Simulation | β | $k_p^0$ L·mol$^{-1}$·s$^{-1}$ | log$M_1$ | log$M_2$ | $L_1^{LIP}/L_2^{LIP}$ | $L_1^{max}$ | $h_2^{inf}/h_1^{max}$ | $g_1^c$ | $g_2^c$ |
|---|---|---|---|---|---|---|---|---|---|---|
| 500 | FM-PREDICI | 0.00 | 15860 | 4.4618 | 4.7486 | 0.517 | 388 | 0.745 | 0.0473 | 0.0726 |
| | FM-PREDICI | 0.05 | 20290 | 4.4505 | 4.7342 | 0.532 | 387 | 0.742 | 0.0486 | 0.0730 |
| | FM-PREDICI | 0.10 | 26000 | 4.4600 | 4.7212 | 0.547 | 386 | 0.743 | 0.0487 | 0.0717 |
| | FM-PREDICI | 0.15 | 33390 | 4.4599 | 4.7109 | 0.561 | 386 | 0.743 | 0.0482 | 0.0700 |
| | AECS | 0.00 | 15350 | 4.4526 | 4.7390 | 0.517 | 387 | 0.743 | 0.0248 | 0.0571 |
| 250 | FM-PREDICI | 0.00 | 15860 | 4.7537 | 5.0337 | 0.525 | 748 | 0.598 | 0.0617 | 0.1034 |
| | FM-PREDICI | 0.05 | 20290 | 4.7388 | 5.0051 | 0.542 | 723 | 0.597 | 0.0633 | 0.1044 |
| | FM-PREDICI | 0.10 | 26000 | 4.7262 | 4.9801 | 0.557 | 702 | 0.602 | 0.0625 | 0.1030 |
| | FM-PREDICI | 0.15 | 33390 | 4.7143 | 4.9572 | 0.572 | 682 | 0.602 | 0.0627 | 0.1018 |
| | AECS | 0.00 | 15230 | 4.7271 | 5.0118 | 0.519 | 714 | 0.600 | 0.0308 | 0.0665 |

**Table S5.** The output values of β estimated by Approach 1 by analysis of the simulated MMDs calculated at 500 and 250 Hz (Figure S9) after using the AECS or FM-PREDICI model (with varying levels of CLD-propagation) to fit the main features of the distribution. The input values of β used to generate the simulated data are provided in the header row.

| | | | FM-PREDICI | | | | AECS |
|---|---|---|---|---|---|---|---|
| p.r.r. (Hz) | Fitting Distribution | Input β: | **0.0** | **0.05** | **0.10** | **0.15** | **0.0** |
| 500 | FM-PREDICI, β = 0.00 | | 0.0085 | 0.0548 | 0.1003 | 0.1459 | 0.0098 |
| | FM-PREDICI, β = 0.05 | | 0.0099 | 0.0563 | 0.1019 | 0.1477 | 0.0112 |
| | FM-PREDICI, β = 0.10 | | 0.0121 | 0.0587 | 0.1046 | 0.1506 | 0.0135 |
| | FM-PREDICI, β = 0.15 | | 0.0141 | 0.0609 | 0.1069 | 0.1532 | 0.0155 |
| | AECS (β = 0.0) | | –0.0013 | 0.0441 | 0.0886 | 0.1333 | 0 |
| 250 | FM-PREDICI, β = 0.00 | | 0.0042 | 0.0523 | 0.1000 | 0.1461 | –0.0113 |
| | FM-PREDICI, β = 0.05 | | 0.0050 | 0.0532 | 0.1009 | 0.1471 | –0.0105 |
| | FM-PREDICI, β = 0.10 | | 0.0061 | 0.0544 | 0.1023 | 0.1486 | –0.0094 |
| | FM-PREDICI, β = 0.15 | | 0.0085 | 0.0570 | 0.1051 | 0.1516 | –0.0072 |
| | AECS (β = 0.0) | | 0.0159 | 0.0651 | 0.1140 | 0.1612 | 0.0000 |

**Table S6.** The output values of β estimated by Approach 2 by analysis of the simulated MMDs calculated at 500 and 250 Hz (Figure S9) after using the AECS or FM-PREDICI model (with varying levels of CLD-propagation) to fit the main features of the distribution. The input values of β used to generate the simulated data are provided in the header row.

| p.r.r. (Hz) | Fitting Distribution | Input β: | **0** | **0.05** | **0.1** | **0.15** |
|---|---|---|---|---|---|---|
| 500 | FM-PREDICI, β = 0.00 | | 0.0000 | 0.0484 | 0.0956 | 0.1426 |
| | FM-PREDICI, β = 0.05 | | 0.0015 | 0.0500 | 0.0973 | 0.1445 |
| | FM-PREDICI, β = 0.10 | | 0.0038 | 0.0525 | 0.1000 | 0.1474 |
| | FM-PREDICI, β = 0.15 | | 0.0058 | 0.0547 | 0.1024 | 0.1500 |
| | AECS (β = 0.0) | | –0.0103 | 0.0373 | 0.0836 | 0.1297 |
| 250 | FM-PREDICI, β = 0.00 | | 0.0000 | 0.0492 | 0.0977 | 0.1445 |
| | FM-PREDICI, β = 0.05 | | 0.0008 | 0.0500 | 0.0986 | 0.1454 |
| | FM-PREDICI, β = 0.10 | | 0.0019 | 0.0513 | 0.1000 | 0.1470 |
| | FM-PREDICI, β = 0.15 | | 0.0043 | 0.0539 | 0.1028 | 0.1500 |
| | AECS (β = 0.0) | | 0.0117 | 0.0620 | 0.1117 | 0.1597 |

**Table S7.** The output values of β estimated by Approach 3 by analysis of the simulated MMDs calculated at 500 and 250 Hz (Figure S9) after using the AECS or FM-PREDICI model (with varying levels of CLD-propagation) to fit the main features of the distribution. The input values of β used to generate the simulated data are provided in the header row.

| | | FM-PREDICI | | | | AECS |
|---|---|---|---|---|---|---|
| Fitting simulation | Input β: | **0.0** | **0.05** | **0.10** | **0.15** | **0.0** |
| FM-PREDICI, β = 0.00 | | 0.0000 | 0.0499 | 0.0998 | 0.1463 | –0.0341 |
| FM-PREDICI, β = 0.05 | | 0.0001 | 0.0500 | 0.0999 | 0.1464 | –0.0341 |
| FM-PREDICI, β = 0.10 | | 0.0002 | 0.0501 | 0.1000 | 0.1465 | –0.0342 |
| FM-PREDICI, β = 0.15 | | 0.0029 | 0.0480 | 0.1032 | 0.1500 | –0.0315 |
| AECS (β = 0.0) | | 0.0336 | 0.0869 | 0.1403 | 0.1905 | 0.0000 |

## 2. Figures

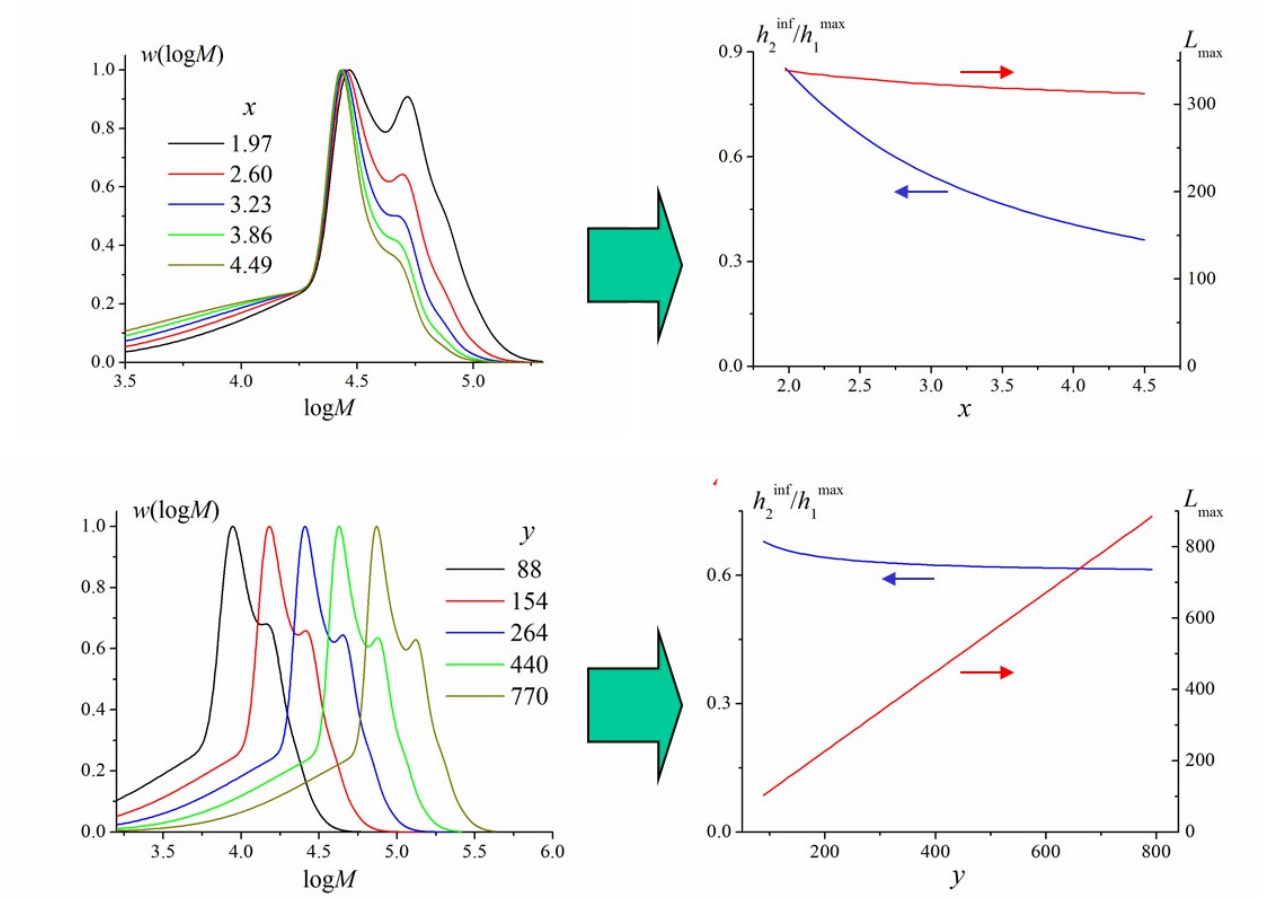


**Figure S1**. The dependencies of peak-normalized MMDs (left) and values of their characteristic features (right) $h_2^{inf}/h_1^{max}$ (blue curves) and $L_{max}$ (red curves) on $x$ and $y$ values, set by varying concentration of radicals produced by a pulse, ρ, and $k_p$ in the AECS simulation of MMDs produced by PLP of MA in bulk at 25 °C. The value of $y$ is set to 290.2 and the value of $x$ is set to 2.62 for the variation in $x$ (top plots) and in $y$ (bottom plots), respectively. Other parameters used for calculation are fixed at δ = 0.1, σ = 0.04, $t_d$ = 0.002 s, [M] = 11.0 mol·L$^{-1}$.

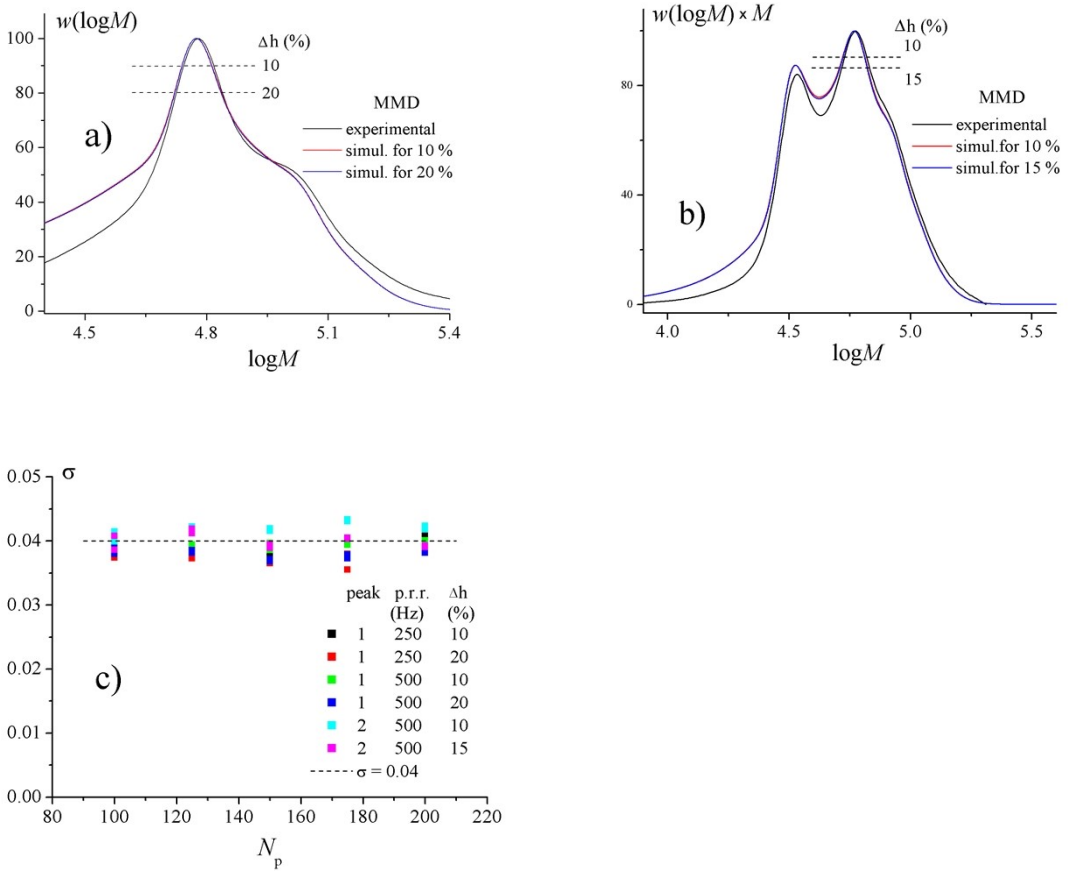


**Figure S2**. The results from the estimation of σ (c) by fitting peak widths at height h = ($h_{max}$ − Δh) for the experimental distributions $w(\log M)$ (a) and $w(\log M)\times M$ (b) by the FM-PREDICI simulation. The principal MMD peak obtained at p.r.r. = 250 Hz and the two peaks observed at p.r.r. 500 Hz are used to estimate σ .

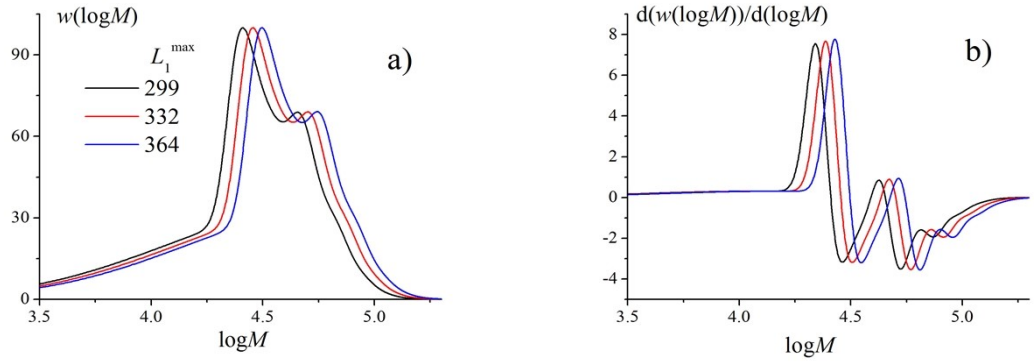


**Figure S3**. Peak-normalized MMDs simulated by the AECS model (a) and corresponding first derivative curves (b) for PLP of bulk MA at 25°C with varying values of $k_p$ and $x$ ($k_p$ = 11 940, 13 290 and 14 600 L·mol$^{-1}$·s$^{-1}$ for black, red and blue curves, respectively; $x$ = 2.480, 2.471 and 2.464 for black, red and blue curves, respectively) that lead to the same value for $h_2^{inf}/h_1^{max}$ = 0.672. These distributions are considered as fits to the MMD (with $h_2^{inf}/h_1^{max}$ = 0.672 and $L_1^{max}$ = 332) calculated by the 3D simulation with [I] = 3 mmol·L$^{-1}$, $E_p$ = 3 mJ and $N_p$ = 100. All simulations were conducted with δ = 0.1, σ = 0.04 and p.r.r. = 500 Hz.

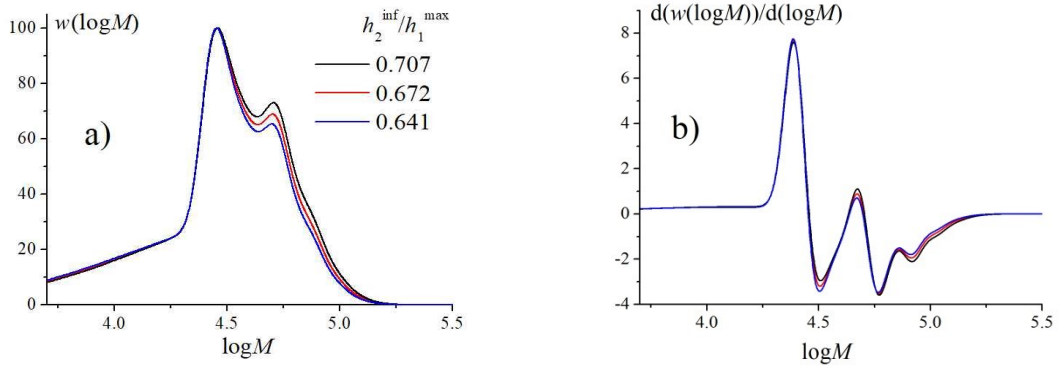


**Figure S4**. Peak-normalized MMDs simulated by the AECS model (a) and corresponding first derivative curves (b) for PLP of bulk MA at 25 °C with $k_p$ = 13 290 L·mol$^{-1}$·s$^{-1}$ and varying values of $x$ ($x$ = 2.585 (black curve), 2.475 (red curve) and 2.360 (blue curve)) that influence the $h_2^{inf}/h_1^{max}$ ratio, as indicated by the legend. These distributions are considered as fits to the MMD calculated by the 3D simulation with [I] = 3 mmol·L$^{-1}$, $E_p$ = 3 mJ and $N_p$ = 100. All simulations were conducted with δ = 0.1, σ = 0.04 and p.r.r. = 500 Hz.

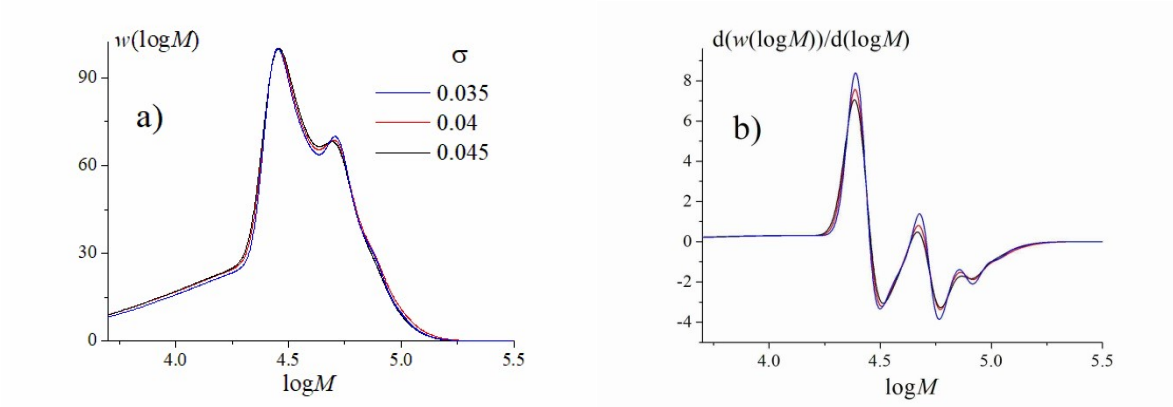


**Figure S5**. Peak-normalized MMDs simulated by the AECS (a) and corresponding first derivative curves (b) for PLP of bulk MA at 25 °C calculated using different values of the SEC broadening parameter (σ) with $k_p$ = 13 290 L·mol$^{-1}$·s$^{-1}$, $x$ = 2.512 (black curve), 2.475 (red curve) and 2.429 (blue curve) set to maintain $h_2^{inf}/h_1^{max}$ = 0.672. These distributions are considered as fits to the MMD calculated by 3D simulation with [I] = 3 mmol·L$^{-1}$, $E_p$ = 3 mJ, $N_p$ = 100 and σ = 0.04. All simulations were conducted with δ = 0.1 and p.r.r. = 500 Hz.

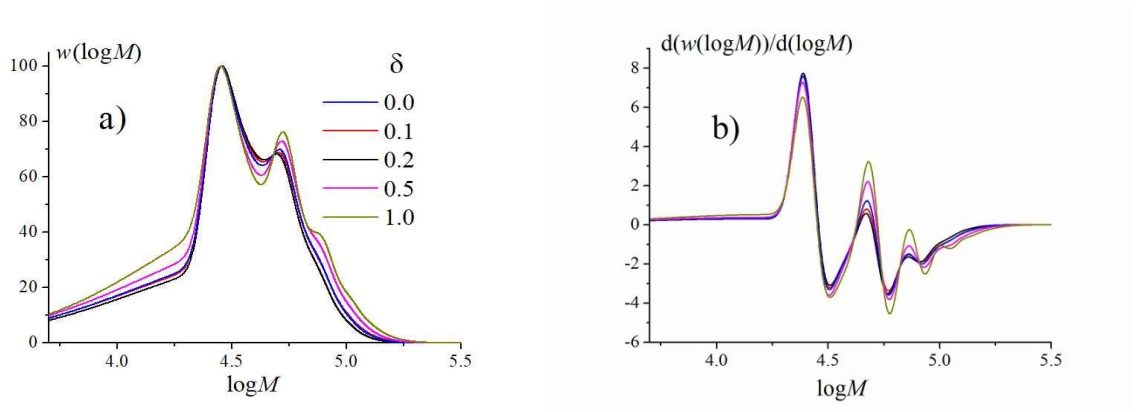


**Figure S6**. Peak-normalized MMDs simulated by the AECS (a) and corresponding first derivative curves (b) for PLP of bulk MA at 25 °C calculated for varying values of the mode of termination (δ) with $k_p$ = 13 290 L·mol$^{-1}$·s$^{-1}$, $x$ = 2.606 (blue curve), 2.475 (red curve), 2.34 (black curve), 1.96 (magenta curve) and 1.474 (dark yellow curve) set to maintain $h_2^{inf}/h_1^{max}$ = 0.672. These distributions are considered as fits to the MMD calculated by the 3D simulation with [I] = 3 mmol·L$^{-1}$, $E_p$ = 3 mJ, δ = 0.1 and $N_p$ = 100. All simulations were conducted with p.r.r. = 500 Hz and σ = 0.04.

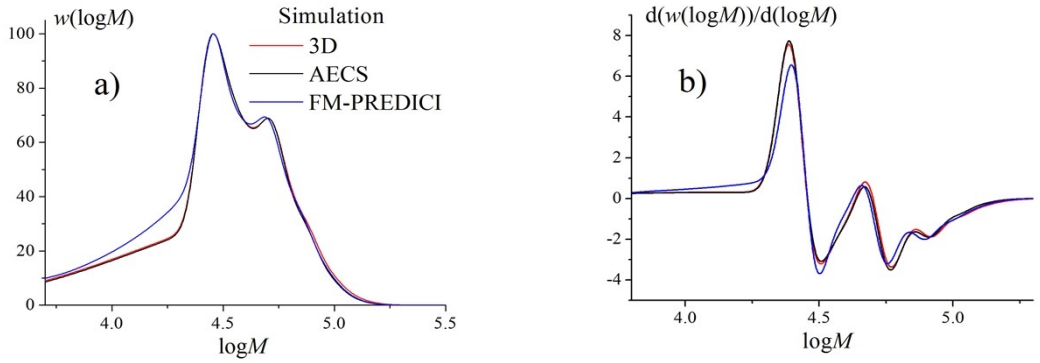


**Figure S7**. Peak-normalized MMDs (a) with corresponding first derivative curves (b) calculated by the FM-PREDICI (blue curve) and the AECS (black curve) models to fit distribution calculated by 3D simulation (red curve) for PLP of bulk MA at 25 °C with σ = 0.04, δ = 0.1 and p.r.r. = 500 Hz. The kinetic parameters used for the AECS calculation were $k_p$ = 13 290 L·mol$^{-1}$·s$^{-1}$ and $x$ = 2.475 and for the FM-PREDICI simulation $k_p^0$ = 22 350 L·mol$^{-1}$·s$^{-1}$, β = 0.10, and ρ = 3.3×10$^{-5}$ mol·L$^{-1}$, with other parameters given in Table S1. For the 3D simulation the kinetic parameters from Table S2 are used with [I] = 3 mmol·L$^{-1}$, $E_p$ = 3 mJ and $N_p$ = 100.

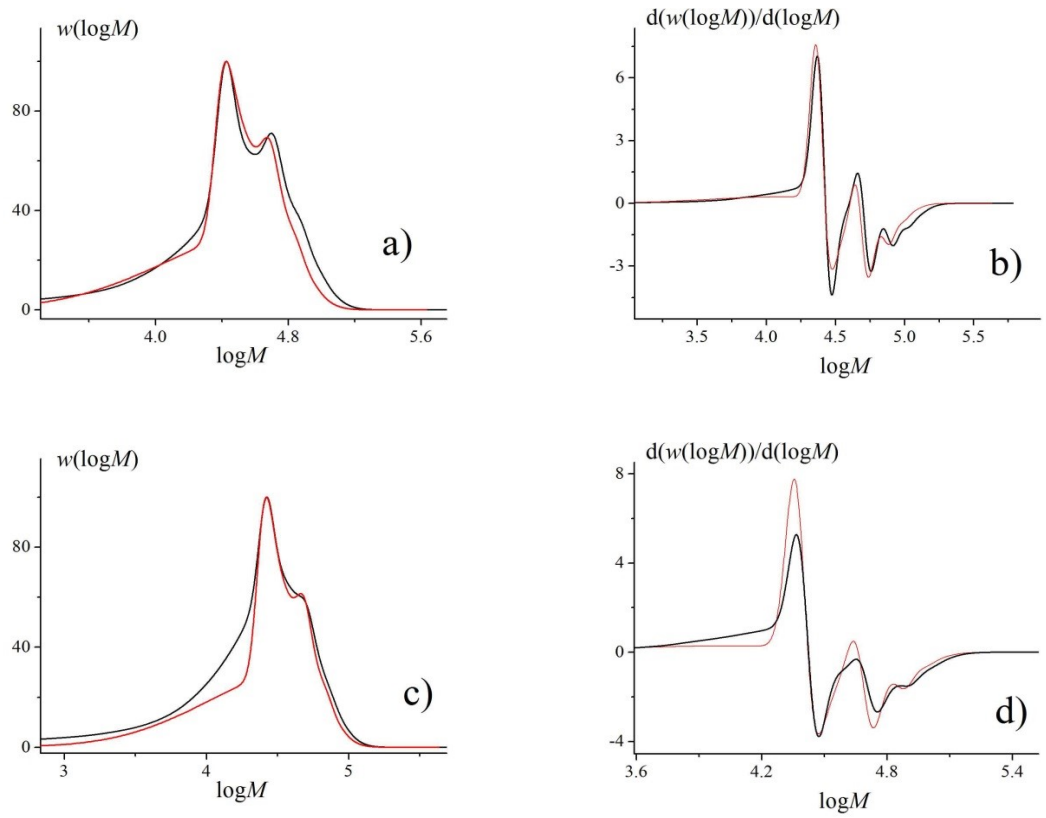


**Figure S8**. Peak-normalized MMDs (a,c) calculated by the FM-PREDICI simulation (black curve) for PLP of bulk MA at 25 °C with corresponding first derivative curves (b,d). The fits by the AECS representation (red curve) reach correspondence in the values of $L_1^{max}$ and $h_2^{inf} / h_1^{max}$ through selection of input values $k_p$ and $x$. Kinetic parameters for the FM-PREDICI simulation are given in Table S1 with $\rho = 4.0 \times 10^{-5}$ mol·L$^{-1}$, $k_p^0 = 13\,190$ L·mol$^{-1}$·s$^{-1}$ and $\beta = 0$ (i.e., no chain length dependence) with the value of $k_{bb}$ set to 229 (a) and 458 s$^{-1}$ (c). The kinetic parameters set to achieve correspondence by the AECS representation were $k_p = 12\,380$ L·mol$^{-1}$·s$^{-1}$, with $x = 2.464$ (a) and 2.725 (c). All simulations were conducted with $\sigma = 0.04$, $\delta = 0.1$ and p.r.r. = 500 Hz.

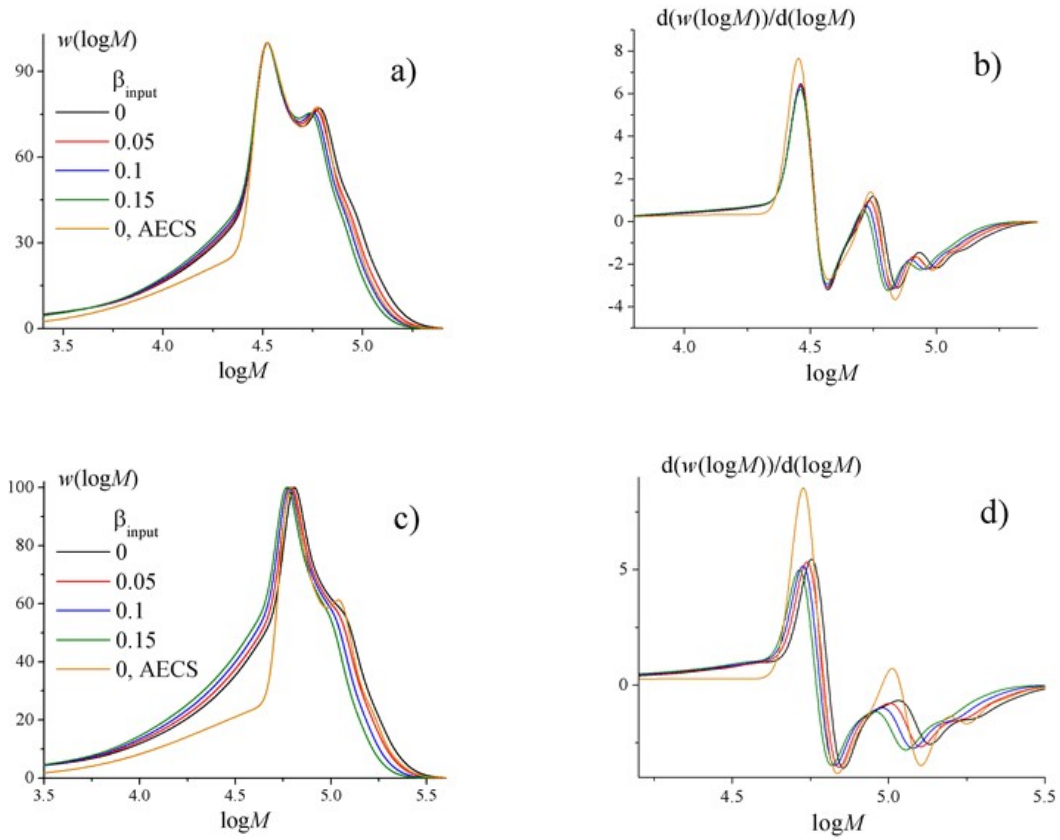


**Figure S9**. MMDs (a,c) and their derivatives (b,d) obtained by the FM-PREDICI and AECS simulations calculated for p.r.r 500 (a,b) and 250 Hz (c,d) to have near-identical $L_1^{max}$ and $h_2^{inf}/h_1^{max}$ at each repetition rate. To reach such correspondence for FM-PREDICI calculations, ρ is chosen to be $2.7\times10^{-5}$, $2.95\times10^{-5}$, $3.05\times10^{-5}$ and $3.1\times10^{-5}$ mol·L$^{-1}$ and $k_p^0$ to be 15 860, 20 290, 26 000 and 33 390 L·mol$^{-1}$·s$^{-1}$ for β = 0, 0.05, 0.1 and 0.15, respectively; other kinetic parameters are given in Table S1. For MMDs calculated by the AECS simulation, $x$ = 2.243 and $k_p$ = 15 350 L·mol$^{-1}$·s$^{-1}$ at 500 Hz, $x$ =2.684 and $k_p$ = 14 530 L·mol$^{-1}$·s$^{-1}$ at 250 Hz were selected. All simulations were conducted with σ = 0.04 and δ = 0.1.

## 3. Details of the *in silico* simulations

### 3.1. Analysis by the 3D simulation

The validity of Approaches 1 and 3 to evaluate CLD $k_p$ parameters is first checked by analysis of the MMDs presented in Figure 2 of the manuscript. Approach 2 could not be used for this check as the 3D simulation is based on analytical expressions,[11] such that $L|_{t=0} = L_p = 0$ (Equation (9)). The fitted $k_p$ values determined by fitting the AECS simulations to MMDs generated using the 3D model for 500 Hz (see Figure 2 of manuscript) are found to be 13 290 and 13 430 L·mol$^{-1}$·s$^{-1}$ for $N_p$ = 100 and 200, respectively, and 13 330 and 13 530 L·mol$^{-1}$·s$^{-1}$ for $N_p$ = 100 and 200, respectively, at 250 Hz. These output values increase with $N_p$ and

decrease with p.r.r. and are slightly higher than the input $k_p$ value of 13 130 L·mol$^{-1}$·s$^{-1}$ used in the 3D simulation. The small difference is associated with the slight increase of temperature in the medium predicted by the 3D simulation that results in an increase of $k_p$.[7] The estimated increase in $k_p$ is not high, no more than 3 %, and does not influence the estimation of β as it influences $L_1$ and $L_2$ values equally. However, the application of an increased $N_p$ above 200 is undesirable, as it may result in reduced accuracy in the estimates of $k_p^0$ values due to spatial inhomogeneities and possible temperature increase due to increased conversion.

With this initial verification of the fitting procedure, additional variations were examined, in each case using the AECS model to fit the output MMD from the 3D simulation calculated with p.r.r. = 500 Hz and $N_p$ = 100. For the base case distribution plotted in Figure 2 of manuscript, values of $L_1^{max} = 332$, $h_2^{inf}/h_1^{max} = 0.672$, $\sigma = 0.04$, and the fraction of termination by disproportionation, $\delta = 0.1$, were assumed. Fitting of MMDs generated with variations in these values allows the evaluation of the influence of possible systematic error in the determination of β and $k_p^0$, with the discussion particularly focused on β. To simplify presentation of the results, only Approach 1 is considered, as systematic errors in estimation of the CLD parameters introduced by this approach are found to be of similar magnitude as for Approach 3.

An insignificant change in the estimated output value of β (≤ 0.001) is observed even if the value of $L_1^{max}$ is purposely poorly fitted by a deviation of 10 % from the input value used in the 3D simulation (Table S3). As shown in Figure S3, the variation in $L_1^{max}$ shifts the entire distribution (and thus the estimate of $k_p^0$) but does not influence the shape. Simulations also show (Figure S4, Table S3) that a ± 5% deviation in the fitted $h_2^{inf}/h_1^{max}$ values does not greatly influence the output estimate of β, which remains equal or less than 0.002, very close to the input value of 0. Based on this result, our experimental MMDs having values of $h_2^{inf}/h_1^{max}$ within ± 5% from each other are grouped together, without any adverse influence on the estimation of β. Furthermore, varying the Gaussian broadening parameter σ from 0.035 to 0.045 does not significantly bias the output value of β, which varies from 0.0074 to −0.0059 (Figure S5, Table S3).

However, it is found that the mode of termination for secondary radicals can influence markedly the estimated CLD parameters for propagation. Figure S6 shows distributions

calculated by the AECS varying δ between zero and unity, but otherwise representing the same 3D distribution (thus all having the value $h_2^{\inf}/h_1^{\max}$ = 0.672 with $L_1^{\max}$ deviating from 332 not more than 1 %) calculated using δ = 0.1. For the higher values of δ = 0.5 and 1.0 (i.e., 50 and 100% termination by disproportionation), the output value of β increases to 0.025 and 0.035, respectively, indicating weak CLD-propagation even though the input value of β was set to zero. However, for δ = 0.5 and 1.0, it is observed that the third peak in the derivative plot calculated from the simulated MMD is more evident than for the curve calculated with δ ≤ 0.2. Moreover, a fourth peak is even seen for δ = 1.0. Such features are not observed in the experimental distributions obtained in this study (Figure 3 of main manuscript), with the shape of the experimental derivative curves very close to the ones obtained for δ ≤ 0.2 in our simulation. Therefore, it is expected that termination of secondary acrylate radicals occurs predominantly by combination, in accord with recent literature.[13] With δ ≤ 0.2 for MA polymerization, the systematical error introduced in the estimate of β is less than 0.01.

This series of simulations has considered the possible influence of various factors on the accuracy of estimating the value of β, including the effect of instationary processes, spatial inhomogeneities and small temperature increases on the PLP-generated MMDs, SEC broadening, uncertainty in the mode of termination, and accuracies in the $L_1^{\max}$ and $h_2^{\inf}/h_1^{\max}$ values estimated by the fitting procedure. According to our analysis, none of these factors adversely influence the estimation procedures we have developed; i.e., in all cases they recovered the correct result of no chain-length dependence. However, this analysis is carried out using the classical scheme of polymerization that does not include actual CLD of propagation and termination, and does not consider the reactions associated with backbiting for methyl acrylate polymerization. The potential effect of these factors on the estimation procedures are considered in the following section.

## 3.2. Analysis by FM-PREDICI simulation

The MMD generated by the 3D model (fitted in Figures 2 and S3-S6) have been refit using the FM-PREDICI model, to determine whether the choice of the model used to fit the distribution can lead to a systematic misrepresentation of CLD-propagation. The kinetic parameters required to fit the MMD simulated at 500 Hz and 100 pulses (Figure 2) were $k_p$ = 13 290 L·mol$^{-1}$·s$^{-1}$ and $x$ = 2.475 when the AECS model was used. In contrast to this simple

representation of PLP, the FM-PREDICI simulation includes both backbiting and CLD-termination, with associated rate coefficients set to literature values (Table S1). The FM-PREDICI simulation also assumes CLD-propagation according to Equation (2), with β set to 0.10 for chain length $L \geq 5$, with the CLD of short chains ($L \leq 5$) represented by Equation (1). The cross-over chain length $L_c = 5$ is chosen in accordance with the procedure outlined in Section 4.2 below. Values of $k_p^0 = 22\,350$ L·mol$^{-1}$·s$^{-1}$ and $\rho = 3.3\times10^{-5}$ mol·L$^{-1}$ are required for the FM-PREDICI model to match the $L_1^{max}$ (= 332) and $h_2^{inf} / h_1^{max}$ (= 0.672) values of the distribution simulated with the 3D model, as shown in Figure S7. This fit is then used to estimate correction factors according to the procedures in Section 4 of the manuscript, before applying Approach 1 to examine for CLD-propagation features of the input distribution generated by the 3D simulation. Although the FM-PREDICI fitting model assumes CLD-propagation with β = 0.10, an output value of 0.016 is estimated for β from analysis of the MMD simulated using the 3D model. Thus, even though the AECS and FM-PREDICI fitting models vary greatly in kinetic complexity, forcing them to match the $L_1^{max}$ and $h_2^{inf} / h_1^{max}$ features of the input distribution (i.e., generated by the 3D model) leads to a reasonable estimation of the importance of CLD-propagation. We have chosen to apply the FM-PREDICI model to fit our MA experimental data, as it takes into account all the important reactions of this polymerization.

In addition, we use simulation to investigate how the presence of backbiting affects the estimation of β by Approach 1. As a first step, the "input" MMDs are calculated by the FM-PREDICI model shown by Scheme S1 and using kinetic parameters from Table S1 without consideration of CLD of $k_p$ of long radicals (i.e., β = 0 is used in simulation) for different values of $k_{bb}$. These simulated MMDs, shown in Figure S8, are then fitted by the AECS model to match $L_1^{max}$ and $h_2^{inf} / h_1^{max}$, after which the output value of β is estimated by Approach 1. The values are found to be –0.02 and –0.007 for $k_{bb}$ = 229 and 458 s$^{-1}$, respectively. Thus, the reactions associated with backbiting have only a minor influence on the estimation of β, even though the two-fold increase in $k_{bb}$ results in a marked change of the shape of distribution, especially at chain lengths below $L_1$ (Figure S8c). Once again, achieving correspondence in the $L_1^{max}$ and $h_2^{inf} / h_1^{max}$ values in the input and fitting distributions provides a robust means to estimate CLD parameters for $k_p$, even in the presence of backbiting.

To complete the *in silico* analysis, both the FM-PREDICI and AECS models have been used to calculate MMDs at p.r.r. values of 250 and 500 Hz, as shown in Figure S9. Four

levels of CLD-propagation are implemented in the FM-PREDICI calculations with β = 0, 0.05, 0.10, and 0.15. For these β values, setting ρ to $2.7\times10^{-5}$, $2.95\times10^{-5}$, $3.05\times10^{-5}$ and $3.1\times10^{-5}$ mol·L$^{-1}$ and $k_p^0$ to 15 860, 20 290, 26 000 and 33 390 L·mol$^{-1}$·s$^{-1}$, respectively, leads to simulated MMDs with identical $L_1^{max}$ (387, with deviation less than 0.4%) and $h_2^{inf}/h_1^{max}$ (0.743, with deviation no greater than 0.3%) values for p.r.r. 500 Hz, with the MMDs and corresponding derivative plots shown in Figure S9a and S9b. The same kinetic parameters are used to simulate the MMDs for p.r.r. 250 Hz presented in Figure S9c, with derivative curves shown in Figure S9d; once again, identical $h_2^{inf}/h_1^{max}$ values (0.600, with deviation no greater than 0.5%) and $L_1^{max}$ values (714, with deviation less than 5 %) are obtained from analysis of the MMDs simulated using the FM-PREDICI model with varying levels of CLD propagation. In addition, the AECS is used to calculate input MMDs without considering any chain-length dependencies or backbiting, with $x$ = 2.243 and $k_p$ = 15 350 L·mol$^{-1}$·s$^{-1}$ for p.r.r. 500 Hz (Figure S9a) and $x$ =2.684 and $k_p$ = 14 530 L·mol$^{-1}$·s$^{-1}$ for p.r.r. 250 Hz (Figure S9c). These kinetic parameters result in $L_1^{max}$ and $h_2^{inf}/h_1^{max}$ values that are the same as the mean values from the MMDs simulated with the FM-PREDICI model with p.r.r of 250 and 500 Hz (Table S4).

An examination of the MMDs plotted in Figure S9a indicates that the position of the 2nd inflection point shifts to lower molar masses with increasing β for p.r.r 500 Hz. The distributions calculated for p.r.r. 250 Hz (Figure S9c) also show a minor shift in the position of the first inflection point, with the shifts of the 2nd inflection point markedly stronger. The resulting increase in the $L_1^{LIP}/L_2^{LIP}$ ratio (see Table S4) is a qualitative indication of the slight decrease in $k_p$ with increasing chain length. For all of the FM-PREDICI simulated distributions, the slight differences between the input $L_i$ values, calculated according to Equation (7a), and the $L_i^{LIP}$ values obtained by differentiating the calculated MMD are used to calculate the correction factors $g_1^c$ and $g_2^c$, also reported in Table S4 for each distribution. Correction factors are also determined from the MMD calculated by the AECS simulation, with $L_i = i k_p[M] t_d$.

Consider the MMDs calculated for p.r.r. 500 Hz shown in Figure S9a. As these distributions all have near-identical values of $L_1^{max}$ and $h_2^{inf}/h_1^{max}$, each can be considered as a suitable representation of the others. For example, the AECS representation (calculated with no backbiting and chain-length dependencies) can be used to fit the FM-PREDICI distribution

calculated with backbiting and strong CLD propagation (with β = 0.15), and vice versa. Thus, the $g_1^c$ and $g_2^c$ factors determined from each of the simulated distribution are applied to estimate β and $k_p^0$ values from the others, to determine if the input chain-length dependencies are correctly recovered. The results of such a check for Approach 1 (i.e., applying Equation (8)) are presented in Table S5, with the input β values indicated as column headers. The rows summarize the corresponding values estimated using a particular application of the model. For the FM-PREDICI distribution calculated without any CLD (i.e., β = 0), Approach 1 yields β estimates ranging between –0.0013 (fit by AECS) and +0.0141 (fit by FM-PREDICI model that assumes strong chain-length dependency). For the majority of the combinations examined, the largest mismatches between input and estimated β values occur when the AECS representation is used to fit the MMDs calculated by the FM-PREDICI model, and when the FM-PREDICI model (that includes backbiting and CLD-termination) is used to fit the MMDs calculated with the AECS model. In the former case, the systematic error in the estimation of β increases to –0.016 as the input value of β increases (i.e., an output value of 0.1333 is calculated for the 0.15 input), and for the latter case the error increases to ~+0.016. For all other cases (i.e., when the more realistic FM-PREDICI representation of MA polymerization is used), the magnitude of the simulated CLD-propagation is recovered using Approach 1, with an error of less than 0.01 in the estimations of β. As also summarized in Table S5, the values of β estimated from the distributions calculated and fit by the FM-PREDICI model with p.r.r. 250 Hz (Figure S9c) exhibit even lower error, although the error for the AECS simulations is slightly increased (and in the opposite direction) compared to the 500 Hz cases.

A closer examination of Table S5 indicates that the value of β is not exactly recovered even when the fitting distribution uses the same level of CLD-dependency for propagation as the simulation. For example, a β value of 0.0563 is estimated when the FM-PREDICI model with β = 0.05 is used to fit the distribution generated with β = 0.05 at 500 Hz. The reason for this small error is that Approach 1 assumes that the chain length $L_p$ defined by Equation (6) is negligible when deriving Equation (8), whereas the correction factors $g_1^c$ and $g_2^c$ are estimated taking into account the CLD of $k_p$ for short radicals (Equation (1), with parameters in Table S1). This minor discrepancy found by the *in silico* analysis should disappear when applying Approach 2, which explicitly accounts for CLD of short radicals. For distributions calculated by the FM-PREDICI simulation with β = 0, 0.05, 0.10 and 0.15 the values of $L_p$ are found to be 4.103, 3.657, 3.233 and 2.761, respectively, according to the procedure described

in Section 4.2. Numerical solutions of Equation (9a) for these values of $L_p$ lead to the exact recovery of the input value of β for the entries along the diagonal of Table S6 for both 500 and 250 Hz, with values on the off-diagonal indicating an error of less than 0.005 in the value of β, that are less than errors found when applying Approach 1.

Finally, as this series of simulations was done for p.r.r. of both 250 and 500 Hz, the MMDs can also be used to test Approach 3 as a method to estimate β and $k_p^0$ according to Equation (10). In this test, the pair of MMDs calculated at 250 and 500 Hz by the FM-PREDICI simulation with a particular value of β (or by the AECS simulation) are used to fit the distributions calculated with all other values of β (or by the AECS simulation). The results from this exercise are presented in Table S7, with the input β values indicated as column headers. The accuracy in the estimations are very similar to those found for Approach 2 applied to the 500 Hz distributions, with the maximum error occurring when the AECS model is used to fit distributions generated by the FM-PREDICI model or vice versa, and the error in β estimations less than 0.004 if the FM-PREDICI simulation with any β is applied to fit data generated with backbiting and CLD-termination. Note that the accuracy of Approach 3, which uses distributions generated at two different p.r.r., was also found to match that of Approach 1 in Section 4.1.

# 4. Theoretical Section

## 4.1. Derivations of the Three Approaches

### 4.1.1. Consideration for Approach 1

Condition $\left|L_p^{1+\beta}\right| << (1+\beta)U_0 t_d$ results in the following simplified version of Equation (7a):

$$L_1^{1+\beta} = (1+\beta)U_0 t_d \tag{S1a}$$

$$L_2^{1+\beta} = 2(1+\beta)U_0 t_d . \tag{S1b}$$

The ratio of $L_2^{1+\beta}$ to $L_1^{1+\beta}$ is 2, resulting in Equation (8a). In addition, substitution of $U_0 = [M]\,k_p^0$ into Equation (S1a) and (S1b) leads to Equation (8b).

### 4.1.2. Consideration for Approach 2

One could rewrite Equation (7a) as follows

$$L_1^{1+\beta} = L_p^{1+\beta} + (1+\beta)U_0 t_d \tag{S2a}$$

$$L_2^{1+\beta} = L_p^{1+\beta} + 2(1+\beta)U_0 t_d . \tag{S2b}$$

Consideration of the difference $2\,L_1^{1+\beta} - L_2^{1+\beta}$ results in Equation (9a), and Equation (9b) is thus determined from Equation (S2a) and (S2b).

### 4.1.3. Consideration for Approach 3

For chain lengths $L_j'$ (j =1 and 2), the following can be derived,

$$L_p^{1+\beta} = 2L_1'^{1+\beta} - L_2'^{1+\beta} \tag{S3}$$

as done above for chain length $L_i$ (i =1 and 2) for Approach 2. Combining Equations (9b) and (S3) leads to Equation (10a). Considering the difference of $L_2^{1+\beta}$ and $L_1^{1+\beta}$ from Equations (S2) leads to the following expression:

$$L_2^{1+\beta} - L_1^{1+\beta} = (1+\beta)U_0 t_d . \tag{S4}$$

which is the basis for Equation (10b). The same procedure is repeated for chain lengths $L_j'$ (j =1 and 2).

## 4.2. Estimation of $L_p$ for Approach 2

Approach 2 assumes that Equation (1) describes the CLD propagation of short radicals and Equation (2) describes the CLD propagation of long radicals. The cross-over chain length $L_c$ is determined by setting the two representations equal at this chain length according to:

$$k_p^{L_c} = k_p \left[ 1 + C_1 \exp\left( -\frac{\ln(2)}{i_{1/2}} \left( L_c - 1 \right) \right) \right] = k_p^0 L_c^{-\beta} \tag{S5}$$

Numerical solution of (S5) gives $L_c$; this chain length is reached at time $t_c$ according to Equation (S6) obtained by integration of Equation (3) for $L \le L_c$ with initial condition $L\big|_{t=0} = 1$ and with $k_p{}^L$ expressed by Equation (1):

$$t_c = \frac{i_{1/2}}{k_p[\mathrm{M}]\ln(2)} \ln\left( \frac{C_1 + 2^{\frac{L_c - 1}{i_{1/2}}}}{C_1 + 1} \right) \tag{S6}$$

Substitution of the $k_p^L$ expression of Equation (2) for $L \ge L_c$ and integration of Equation (3) with the initial condition $L\big|_{t=t_c} = L_c$ results in:

$$L = \left( L_c^{1+\beta} + (1+\beta) U_0 (t - t_c) \right)^{1/(1+\beta)} \tag{S7}$$

According to (S7) $L_p = L\big|_{t=0}$ could be estimated from (S8)

$$L_p^{1+\beta} = L_c^{1+\beta} - (1+\beta) U_0 t_c \tag{S8}$$

## 4.3. Uncertainties in the estimation of β by the approaches

Consider the estimation of β by Approach 3. For other two approaches the mathematical considerations used to consider accuracy are similar and simpler. Equation (10a) could be rewritten as

$$L_1^{1+\beta} \left( 2 - \left( \frac{L_2}{L_1} \right)^{1+\beta} \right) = L_1'^{1+\beta} \left( 2 - \left( \frac{L_2'}{L_1'} \right)^{1+\beta} \right) \tag{S9}$$

or

$$\left( 2 - \left( \frac{L_2}{L_1} \right)^{1+\beta} \right) = \left( \frac{L_1'}{L_1} \right)^{1+\beta} \left( 2 - \left( \frac{L_2'}{L_1'} \right)^{1+\beta} \right) \tag{S10}$$

Designating $a = L_2/L_1$, $b = L'_2/ L'_1$, $c = L'_1/ L_1$ we have four parameters connected by the relation:

$$\left( 2 - a^{1+\beta} \right) = c^{1+\beta} \left( 2 - b^{1+\beta} \right) \tag{S11}$$

As the differentials on the left and right sides of Equation (S11) are equal, the following expression can be derived:

$$-(1+\beta)a^{\beta}\mathrm{d}a - a^{1+\beta}\ln(a)\mathrm{d}\beta = \\ = (2-b^{1+\beta})(1+\beta)c^{\beta}\mathrm{d}c + c^{1+\beta}\ln(c)(2-b^{1+\beta})\mathrm{d}\beta - \\ -(c^{1+\beta}(1+\beta)b^{\beta}\mathrm{d}b + c^{1+\beta}b^{1+\beta}\ln(b)\mathrm{d}\beta) \quad \text{(S12)}$$

From Equation (S12) we have

$$\mathrm{d}\beta = \frac{(1+\beta)a^{\beta}}{V}\mathrm{d}a - \frac{c^{1+\beta}(1+\beta)b^{\beta}}{V}\mathrm{d}b + \frac{(2-b^{1+\beta})(1+\beta)c^{\beta}}{V}\mathrm{d}c \quad \text{(S13)}$$

$$V = -a^{1+\beta}\ln(a) + c^{1+\beta}b^{1+\beta}\ln(b) - c^{1+\beta}\ln(c)(2-b^{1+\beta}) \quad \text{(S14)}$$

According to Equation (S13), the error associated with the estimation of β by Approach 3 is mainly dependent on the ratios of chain lengths *a* and *b*. Note that the third term in Equation (S13) contains the multiplier $2–b^{1+\beta}$, whose value is expected to be low, thus decreasing the contribution of this term to the error estimated in β.

## References


[1] M. Wulkow, *Macromol. React. Eng.* **2008**, *2*, 461.

[2] H. Kattner, M. Buback, *Macromolecules* **2018**, *51*, 25.

[3] A. N. Nikitin, R. A. Hutchinson, G. A. Kalfas, J. R. Richards, C. Bruni, *Macromol. Theory Simul.* **2009**, *18*, 247.

[4] Y. W. Marien, P. H. M. Van Steenberge, C. Barner-Kowollik, M.-F. Reyniers, G. B. Marin, D. R. D'hooge, *Macromolecules* **2017,** 50, 1371

[5] J. J. Haven, J. Vandenbergh, R. Kurita, J. Gruber, T. Junkers, *Polym. Chem.* **2015**, *6*, 5752.

[6] C. Barner-Kowollik, S. Beuermann, M. Buback, P. Castignolles, B. Charleux, M. L. Coote, R. A. Hutchinson, T. Junkers, I. Lacík, G. T. Russell, M. Stach, A. M. van Herk, *Polym. Chem.* **2014**, *5*, 204.

[7] A. N. Nikitin, I. Lacík, R. A. Hutchinson, *Macromolecules* **2016**, *49*, 9320.

[8] Methyl Acrylate. http://www2.basf.us/acrylicmonomers/pdfs/methacry.pdf, accessed: June 2019.

[9] Methyl acrylate, https://cameochemicals.noaa.gov/chris/MAM.pdf

[10] M. Buback, A. Kuelpmann, C. Kurz, *Macromol. Chem. Phys.* **2002**, *203*, 1065.

[11] A. N. Nikitin, P. Castignolles, B. Charleux, J-P. Vairon, *Macromol. Theory Simul.* **2003,** *12,* 440.

[12] A. N. Nikitin, I. Lacík, R. A. Hutchinson, M. Buback, G.T. Russell, *Macromolecules* **2019**, *52*, 55.

[13] T. G. Ribelli, K. F. Augustine, M. Fantin, P. Krys, R. Poli, K. Matyjaszewski, *Macromolecules* **2017**, *50*, 7920.